Arsenic Effects and Behavior in Association with the Fe(II)-Catalyzed Transformation of Schwertmannite

ARTICLE *in* ENVIRONMENTAL SCIENCE AND TECHNOLOGY · FEBRUARY 2010

Impact Factor: 5.33 · DOI: 10.1021/es903424h · Source: PubMed

6 AUTHORS, INCLUDING:

Edward D Burton
Southern Cross University
144 PUBLICATIONS **1,815** CITATIONS
SEE PROFILE

Kym M Watling
Griffith University
37 PUBLICATIONS **366** CITATIONS
SEE PROFILE

Richard T Bush
Southern Cross University
150 PUBLICATIONS **1,814** CITATIONS
SEE PROFILE

Annabelle F Keene
Southern Cross University
55 PUBLICATIONS **589** CITATIONS
SEE PROFILE

Environ. Sci. Technol. **2010,** *44,* 2016–2021

Arsenic Effects and Behavior in Association with the Fe(II)-Catalyzed Transformation of Schwertmannite

EDWARD D. BURTON,* SCOTT G. JOHNSTON, KYM WATLING, RICHARD T. BUSH, ANNABELLE F. KEENE, AND LEIGH A. SULLIVAN

Southern Cross GeoScience, Southern Cross University, Lismore, New South Wales 2480, Australia

Received November 10, 2009. Revised manuscript received January 20, 2010. Accepted February 1, 2010.

In acid-mine drainage and acid-sulfate soil environments, the cycling of Fe and As are often linked to the formation and fate of schwertmannite ($Fe_8O_8(OH)_{8-2x}(SO_4)_x$). When schwertmannite-rich material is subjected to near-neutral Fe(III)-reducing conditions (e.g., in reflooded acid-sulfate soils or mining-lake sediments), the resulting Fe(II) can catalyze transformation of schwertmannite to goethite. This work examines the effects of arsenic(V) and arsenic(III) on the Fe(II)-catalyzed transformation of schwertmannite and investigates the associated consequences of this mineral transformation for arsenic mobilization. A series of 9-day anoxic transformation experiments were conducted with synthetic schwertmannite and various additions of Fe(II), As(III), and As(V). X-ray diffraction (XRD) and Fe K-edge extended X-ray absorption fine structure (EXAFS) spectroscopy demonstrated that, in the absence of Fe(II), schwertmannite persisted as the dominant mineral phase. Under arsenic-free conditions, 10 mM Fe(II) catalyzed rapid and complete transformation of schwertmannite to goethite. However, the magnitude of Fe(II)-catalyzed transformation decreased to 72% in the presence of 1 mM As(III) and to only 6% in the presence of 1 mM As(V). This partial Fe(II)-catalyzed transformation of As(III)-sorbed schwertmannite did not cause considerable As(III) desorption. In contrast, the formation of goethite via partial transformation of As(III)- and As(V)-sorbed schwertmannite significantly decreased arsenic mobilization under Fe(III)-reducing conditions. This implies that the Fe(II)-catalyzed transformation of schwertmannite to goethite may help to stabilize solid-phase arsenic and retard its subsequent release to groundwater.

Introduction

Schwertmannite is typically the first Fe(III) mineral to precipitate in Fe- and SO_4^{2-}-rich waters within the pH range of 3−4 (*1*). It is widespread in systems affected by acid-mine drainage (AMD) and acid-sulfate soils (ASS) (*2*−*8*). Such systems are often enriched in arsenic—a potentially toxic metalloid, which interacts strongly with schwertmannite via sorption−desorption reactions (*9*−*11*). For this reason, the mobility and fate of arsenic can be greatly affected by processes that alter the abundance of schwertmannite (*4, 12*−*15*).

* Corresponding author e-mail: ed.burton@scu.edu.au.

With few exceptions (*16*), field studies and laboratory experiments demonstrate that over time schwertmannite transforms to goethite via a progressive dissolution−precipitation process (*2, 4*−*8, 12*−*15, 17*−*22*). Most studies of schwertmannite transformation have examined oxic and acidic conditions, where the transformation process has been found to be relatively slow, requiring months to years for completion (*2, 4, 5, 7, 19*). However, recent research shows that at pH > 5 in the presence of mM concentrations of Fe(II), the transformation process is accelerated, relative to an absence of Fe(II), by several orders of magnitude (*20, 21*).

Schwertmannite transformation via the Fe(II)-pathway occurs under anoxic, Fe(III)-reducing conditions, where bacterial production of HCO_3^- drives the development of near-neutral pH (*20, 21*). Burton et al. (*20*−*22*) presented field- and laboratory-based evidence on the importance of this transformation pathway in ASS materials, including drain sediments and reflooded soils. Likewise, Johnston et al. (*23*) found iron mineralogy trends in an ASS wetland that were broadly consistent with the Fe(II)-catalyzed transformation of schwertmannite to goethite. Conditions that are conducive to this transformation pathway also occur in a range of AMD situations, such as mine-pit lake sediments and organic-rich constructed wetland soils (*18, 24, 25*). For example, Peine et al. (*18*) found that schwertmannite transformed to goethite following the onset of near-neutral pH in Fe(II)-rich sediments of a lignite mine-pit lake.

In natural waters, arsenic exists predominantly as oxyanions of the arsenic(III) and arsenic(V) oxidation states. Arsenic(V) is known to retard the slow transformation of schwertmannite to goethite under oxic conditions (*4, 26*). Under these conditions, Acero et al. (*12*) found that the transformation of schwertmannite to goethite over a period of about 1 year triggered desorption of previously bound arsenic(V). Nevertheless, Acero et al. (*12*) found, in agreement with Schroth and Parnell (*14*), that the vast majority of arsenic(V) remained associated with the solid-phase (i.e., goethite) following schwertmannite transformation.

While these previous studies provide insight into arsenic(V) fate and schwertmannite transformation under oxic conditions, the effect of either arsenic(V) or arsenic(III) on schwertmannite transformation via the anoxic Fe(II)-pathway has not been examined previously. Likewise, the implications of this transformation pathway for the mobility and fate of schwertmannite-sorbed arsenic has not been addressed. These issues represent important knowledge-gaps with regard to schwertmannite fate and the associated behavior of arsenic in many ASS- and AMD-affected environments.

Here we examine the effect of both arsenic(V) and arsenic(III) on schwertmannite transformation via the Fe(II) pathway. We also examine consequences associated with this mineral transformation for arsenic desorption behavior. To achieve these dual objectives, we conducted a series of 9-day anoxic transformation experiments involving synthetic schwertmannite.

Methods

General Methods. All laboratory glass- and plastic-ware was cleaned by soaking in 5% (v/v) HNO_3 for at least 24 h, followed by repeated rinsing with deionized water. All chemicals were analytical reagent grade, and all reagent solutions were prepared with deionized water (Milli-Q). Results for solid-phase analyses are presented on a dry weight basis, unless noted otherwise.

Schwertmannite Synthesis. Schwertmannite was synthesized by H_2O_2 oxidation of a $FeSO_4$ solution (*5*). The

10.1021/es903424h
Published on Web 02/11/2010

TABLE 1. Details of Experimental Treatments and Selected Results for Material at the End of the 9-Day Transformation Experiments

experimental treatments			Fe EXAFS results			sulfate release[a]	As XPS results			intrinsic reactivity		
run I.D.	As	Fe(II)	schwert (%)	goethite (%)	R-factor	(%)	As(III)(%)	As(V) (%)	goodness-of-fit	$\log_{10} k'$ (s^{-1})	γ	r^2
1	none	none	92	8	0.039	13	–	–	–	−4.34	1.00	0.998
2	none	10 mM	3	97	0.008	100	–	–	–	−6.37	1.23	0.640
3	1 mM As(III)	none	100	0	0.028	17	70	30	164	−4.34	1.00	0.969
4	1 mM As(III)	10 mM	28	72	0.040	77	66	34	141	−5.08	1.02	0.963
5	1 mM As(V)	none	100	0	0.081	4	0	100	226	−4.20	1.16	0.996
6	1 mM As(V)	10 mM	94	6	0.056	19	0	100	187	−4.28	1.19	0.997

[a] Sulfate release is expressed as the increase between the initial pre-equilibrated concentrations and the maximum possible concentrations (which are based on the initial solid-phase sulfate concentrations bound within the schwertmannite structure).

resulting schwertmannite suspension was adjusted to pH 3.0 using 1 M NaOH and allowed to settle, and the supernatant was replaced with deionized water. This rinsing procedure was repeated 3 times in order to remove soluble ions, prior to freeze-drying the final concentrated slurry. The mineralogy of the dry product was verified using X-ray diffractometry (XRD) as described below. Digestion of the schwertmannite according to Burton et al. (*21*) followed by analysis of Fe and SO_4^{2-} revealed 7.9 mmol g^{-1} Fe(III) and 1.9 mmol g^{-1} SO_4^{2-}, thereby suggesting a composition of $Fe_8O_8(OH)_{4.2}(SO_4)_{1.9}\cdot 10H_2O$.

Transformation Experiments. A series of experiments was conducted at room temperature (20 ± 1 °C) under well-mixed anoxic conditions (achieved by continuous purging with high-purity N_2) in gastight Pyrex reactors. All experimental runs involved 5 g of schwertmannite suspended in 1 L of 0.1 M NaCl, buffered at pH 6.5 using 0.05 M of MES/MOPS (2-morpholinopropanesulfonic and 2-morpholinoethanesulfonic acid). Depending on the experimental treatment (see Table 1), the buffered 0.1 M NaCl background solution contained either no arsenic (runs 1 and 2), 1 mM As(III) (runs 3 and 4), or 1 mM As(V) (runs 5 and 6). The As(V) and As(III) concentrations were achieved by dilution of freshly prepared 1 M solutions of $Na_2HAs^{V}O_4\cdot 0.7H_2O$ and $NaAs^{III}O_2$, respectively.

The experimental runs (performed in duplicate) were initiated by addition of 5 g of schwertmannite to 1 L of deoxygenated background solution held within the Pyrex reactors. The reactors were then sealed and purged with N_2 for 24 h in order to deoxygenate the solution and achieve pre-equilibration with regard to the solid/solution partitioning of SO_4^{2-} and arsenic (*9, 10, 21*). After this initial pre-equilibration period, a small volume (10.1 mL) of deoxygenated 0.1 M NaCl containing either 1 M Fe(II) (prepared immediately before use from $FeCl_2\cdot 4H_2O$) or no Fe(II) was injected into the reactor. Experimental runs 2, 4, and 6 received the Fe(II) addition (initial concentration = 10 mM), while runs 1, 3, and 5 did not receive Fe(II). Additional quality-assurance reactors (which lacked schwertmannite but contained deoxygenated background solution and the same various additions of Fe(II), As(III), and As(V)) demonstrated that aqueous Fe(II) and arsenic concentrations remained constant in the absence of schwertmannite.

At 0, 0.25, 1, 2, 3, 4, 5, 6, 7, 8, and 9 days after the initial pre-equilibration period, 20 mL of the well-mixed suspension was retrieved using a syringe attached to a gastight sampling port. The suspension was filtered to <0.45 μm and immediately acidified to pH < 2 with HCl. At the end of the 9-day reaction, the remaining suspension was centrifuged, with the solid-phase rinsed with deoxygenated water and dried under high-purity N_2.

Analytical Methods. Determination of pH, Fe, SO_4^{2-}, and total aqueous As involved standard methods as described previously (*22*). Aqueous As(V) was determined via a spectrophotometric method (*27*), with As(III) estimated as the difference between total aqueous As and As(V).

Mineralogy was qualitatively determined by X-ray diffraction (XRD) using a Bruker D4 Endeavor fitted with a Co X-ray source and Lynx-Eye detector. Samples were scanned from 10−80° 2θ with a 0.05° 2θ step-size and a 4 s count-time. The XRD patterns were evaluated using EVA software (DIFFRAC-plus evaluation package, Bruker AXS, Karlsruhe, Germany).

In addition to qualitative identification of mineralogy via XRD, the iron speciation in solid-phase samples collected at the end of the transformation experiments was quantified by Fe K-edge extended X-ray absorption fine structure (EXAFS) spectroscopy. The EXAFS data were collected on beamline 17C at the National Synchrotron Radiation Research Centre (NSRRC) in Taiwan. The X-ray energy was calibrated against an in-line Fe(0) foil. Duplicate spectra were collected in fluorescence mode using an ionization chamber. The Athena program was used for standard background subtraction and edge-height normalization using the AUTOBK algorithm (*28*). Iron speciation in the experimental samples was quantified by linear combination fitting of the k^3-weighted EXAFS oscillations in the 2−12 $Å^{-1}$ range, using schwertmannite and goethite (i.e., the only minerals present according to XRD) as reference standards.

The oxidation state of solid-phase arsenic was characterized by X-ray photoelectron spectroscopy (XPS) using a Kratos Axis Ultra HSA XPS with monochromated Al K_α X-rays. Broad scans were obtained using a 160 eV pass energy, while narrow high-resolution scans of the As 3d region were obtained using 20 eV pass energy. The samples were charge neutralized and referenced to adventitious C 1s contamination at 285.0 eV. Spectra were fitted in CasaXPS using a Marquardt optimization and an 80% Gaussian - 20% Lorentzian peak shape after subtraction of a Shirley baseline. The component peaks were identified by comparing binding energies with literature values (*29*). Arsenic-3*d* spectra were fitted with the doublets of $3d_{5/2}$ and 3 $d_{3/2}$ peaks with a spin−orbit splitting of 0.70 eV (*29*). The As $3d_{3/2}$ peak was constrained to be 2/3 the area of the As 3*d*5/2 peak, and the full width at half-maximum (fwhm) of all peak components were also constrained within ranges reported in the literature (*29*).

The susceptibility of the Fe(III) solid-phase to reductive dissolution was quantified using the kinetic approach of Larsen and Postma (*30*). This method involves reductive dissolution in pH 3, 10 mM ascorbic acid, and is widely used to characterize the intrinsic reactivity of Fe(III)-oxides (*31*).

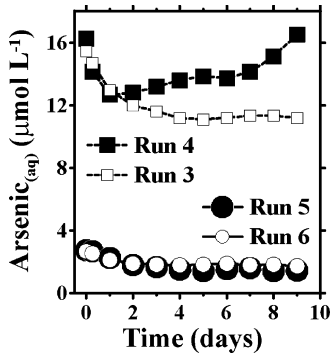

FIGURE 1. Changes in aqueous arsenic concentrations in runs 3 and 4, which initially contained 1 mM As(III), and in runs 5 and 6, which initially contained 1 mM As(V).

Results and Discussion

Sorption of As(V) and As(III) during the Initial Pre-Equilibration Period. After pre-equilibration with 5 g L^{-1} schwertmannite for 24 h, the initial 1 mM aqueous arsenic concentration had decreased to 15.8 ± 0.6 μM As(III) in runs 3 and 4 (Figure 1) and 2.71 ± 0.05 μM As(V) in runs 5 and 6 (Figure 1). These pre-equilibrated concentrations equate to removal of >98% of the added arsenic via sorptive interactions with the schwertmannite solid-phase. As a consequence of this large proportional sorption of added arsenic, the solid-phase arsenic concentrations were very similar for both the As(V) and As(III) experimental runs (i.e., 25.2 $mmol_{As(V)}$ $mol_{Fe(III)}^{-1}$ and 24.9 $mmol_{As(III)}$ $mol_{Fe(III)}^{-1}$, respectively).

There was considerable desorption of schwertmannite-bound SO_4^{2-} during the initial pre-equilibration period. In runs 1 and 2, which did not contain arsenic, the pre-equilibrated SO_4^{2-} concentrations were 5.61 ± 0.24 mM and 5.78 ± 0.46 mM, respectively (Figure 2). This reflects dissolution of 59−61% of the initial solid-phase SO_4^{2-}, which equates to a pre-equilibrated schwertmannite composition of $Fe_8O_8(OH)_{6.48}(SO_4)_{0.76}\cdot nH_2O$. Similar short-term loss of schwertmannite-bound SO_4^{2-} without simultaneous mineralogical transformation has been observed previously as a result of pH-dependent SO_4^{2-} desorption (*7, 21*).

The pre-equilibrated SO_4^{2-} concentrations in runs 3 and 4 (containing As(III)) were 5.88 ± 0.26 mM and 6.06 ± 0.19 mM, respectively (Figure 2). The corresponding SO_4^{2-} concentrations in runs 5 and 6 (containing As(V)) were 6.33 ± 0.18 mM and 6.27 ± 0.16 mM, respectively (Figure 2). These levels of SO_4^{2-} desorption imply that the pre-equilibrated schwertmannite compositions were $Fe_8O_8(OH)_{6.62}(SO_4)_{0.69}\cdot nH_2O$ in the As(III) systems (runs 3 and 4) and $Fe_8O_8(OH)_{6.72}(SO_4)_{0.64}\cdot nH_2O$ in the As(V) systems (runs 5 and 6). The slightly lower solid-phase SO_4^{2-} content in the As(V)- and As(III)-sorbed schwertmannite, compared to the As-free schwertmannite, is consistent with Burton et al. (*11*). These researchers found that both arsenic(V) and arsenic(III) sorption to schwertmannite occurs by incorporation into the solid-phase partly via arsenic exchange for structural SO_4^{2-} groups (*11*).

Effects of Arsenic on Schwertmannite Transformation. Following the initial 24 h pre-equilibration period, the schwertmannite suspensions were allowed to react for 9 days either in the presence or absence of 10 mM Fe(II). At the conclusion of this period, XRD showed that in the absence of Fe(II) (runs 1, 3, and 5) schwertmannite remained the predominant mineral (Figure 3). Linear combination Fe EXAFS confirmed this persistence of schwertmannite, revealing that after 9 days schwertmannite comprised 92% of solid-phase Fe in run 1 and 100% in both runs 3 and 5 (Figure 4, Table 1). The relatively minor goethite formation in run 1 was also evident in the corresponding XRD pattern, which has a small peak corresponding to the (110) Bragg reflection for goethite (Figure 3).

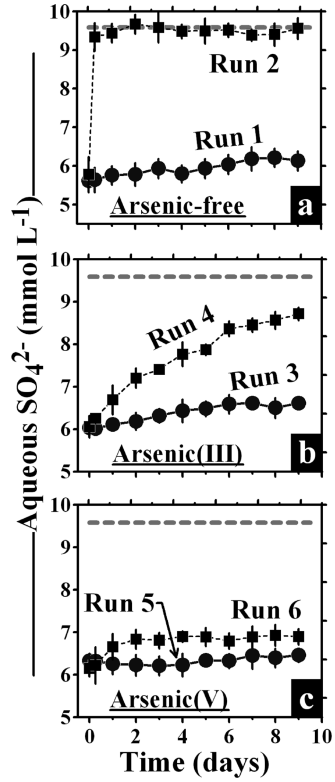

FIGURE 2. Changes in aqueous SO_4^{2-} concentrations over time in (a) runs 1 and 2, (b) runs 3 and 4, and (c) runs 5 and 6. The dashed lines denotes the maximum possible aqueous SO_4^{2-} concentrations based on the initial schwertmannite-bound SO_4^{2-} concentration.

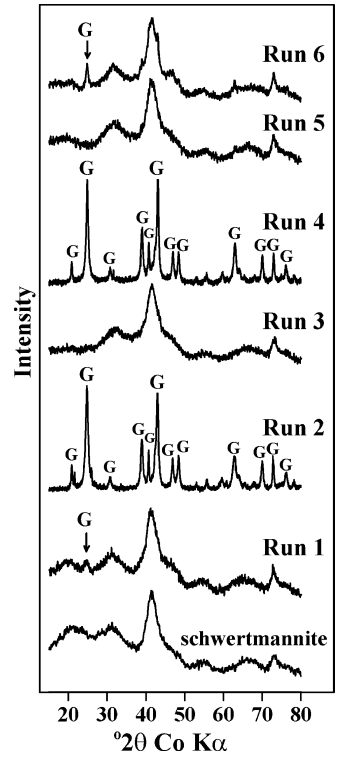

FIGURE 3. X-ray diffractograms of the initial schwertmannite and of solid-phase material at the end of the 9-day reaction period in runs 1−6. The label "G" donotes goethite peaks.

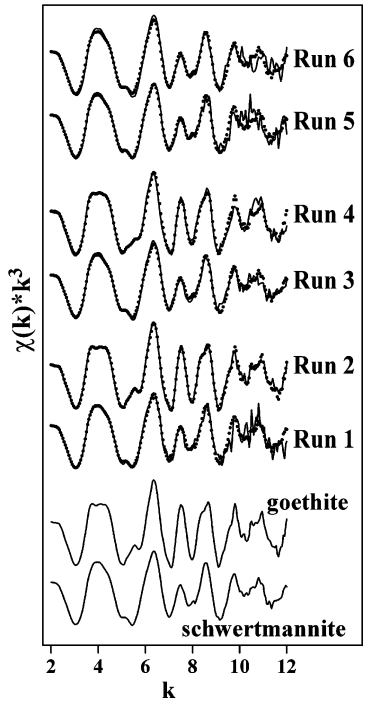

FIGURE 4. k^3-weighted Fe EXAFS spectra for schwertmannite, goethite, and experimental samples collected from runs 1−6. The solid line denotes data, while the dotted line for runs 1−6 shows the linear combination fit.

In contrast to run 1, the presence of 10 mM Fe(II) in run 2 (which was also arsenic-free) catalyzed transformation of the initial schwertmannite to goethite (Figure 3). In quantitative terms, the Fe EXAFS data indicates that the final solid-phase Fe speciation in run 2 comprised 97% goethite and only 3% schwertmannite (Table 1). This agrees with earlier work showing that Fe(II) catalyzes the fast transformation of schwertmannite to goethite (*20, 21*).

The XRD patterns and Fe EXAFS data show that arsenic retarded the Fe(II)-catalyzed transformation of schwertmannite (Figures 3 and 4). Importantly, the degree of this retardation was dependent on the arsenic oxidation state. In the presence of As(V) (i.e., run 6), there was minor Fe(II)-catalyzed transformation of schwertmannite, with only 6% of solid-phase Fe existing as goethite at the end of the reaction period (Table 1). In contrast, in the presence of As(III) (i.e., run 4), there was substantial Fe(II)-catalyzed transformation, with goethite making up 72% of the final solid-phase Fe (Table 1).

The transformation of schwertmannite to goethite causes the expulsion of solid-phase SO_4^{2-} according to (*5, 21*)

$$Fe_8O_8(OH)_{8-2x}(SO_4)_x + 2xH_2O \rightarrow 8FeOOH + xSO_4^{2-} + 2xH^+ \quad (1)$$

Therefore, schwertmannite transformation to goethite can also be estimated from the relative increase in aqueous SO_4^{2-} between the initial pre-equilibrated concentrations and the maximum possible concentrations (Figure 2). The extent of this SO_4^{2-} release over the reaction period is presented in Table 1. The magnitude of SO_4^{2-} release equates to levels of schwertmannite transformation that are 4% to 17% greater than the corresponding Fe EXAFS results (Table 1). This difference may be due to relatively slow desorption of SO_4^{2-} from the schwertmannite solid-phase, driven by solid-solution disequilibrium rather than by an intrinsic mineral transformation (*11, 21*). Nevertheless, in qualitative terms, both the SO_4^{2-} release approach and the Fe EXAFS approach gave broadly comparable estimates of schwertmannite transformation (Table 1).

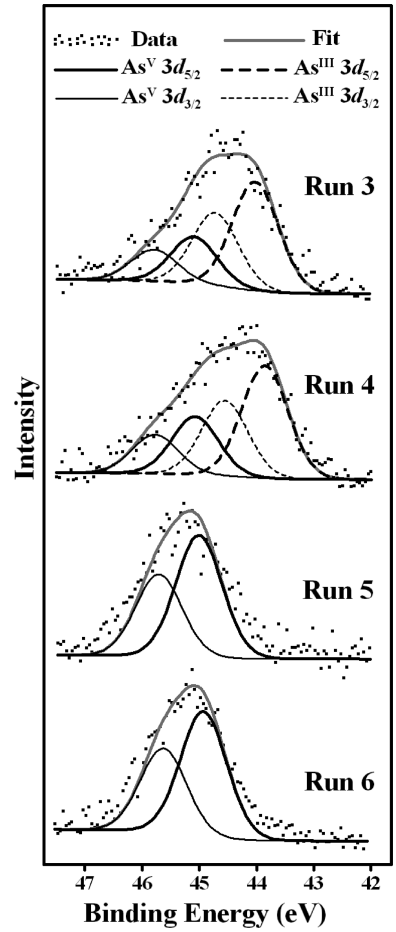

FIGURE 5. Arsenic 3d XPS spectra for the solid-phase material at the end of the 9-day reaction period in runs 3−6.

The distinct difference in degrees of Fe(II)-catalyzed schwertmannite transformation between runs 4 and 6 can be primarily attributed to the contrasting effects of sorbed As(III) and As(V), respectively. However, in the experiments described here, there was potential for As(III) oxidation by Fe(III) and As(V) reduction by added Fe(II). It is therefore important to evaluate if such arsenic redox transformations actually occurred to any substantial extent during the reaction period. Aqueous As(V) was undetectable in runs 3 and 4, and aqueous As(III) was undetectable in runs 5 and 6, which together indicate no change in the aqueous arsenic oxidation state. To further evaluate potential arsenic redox transformations, the oxidation state of solid-phase arsenic in runs 3−6 were quantified by XPS (Figure 5). The results indicate that there was 30−34% oxidation of As(III) in the solid-phase resulting from runs 3 and 4 and no reduction of As(V) in runs 5 and 6 (Table 1). Therefore, while some As(III) oxidation did occur, the XPS results demonstrate that the dominant arsenic oxidation state did not change dramatically during the transformation experiments.

Solid-Solution Partitioning Behavior of Arsenic. In runs 3 and 5, which contained As(III) and As(V), respectively (but did not contain Fe(II)), aqueous arsenic decreased steadily over the first 2−4 days (Figure 1). After this period, the aqueous arsenic concentrations remained relatively constant at 11.1−11.3 μM As(III) in run 3 and at 1.4−1.6 μM As(V) in run 5 (Figure 1). The initial decrease in aqueous As(V) and As(III) can be attributed to relatively slow sorption over the initial few days, as also observed by Burton et al. (*11*).

The Fe(II)-catalyzed transformation of As(III)-sorbed schwertmannite in run 4 caused some As(III) desorption. For example, at the end of the reaction period, the aqueous

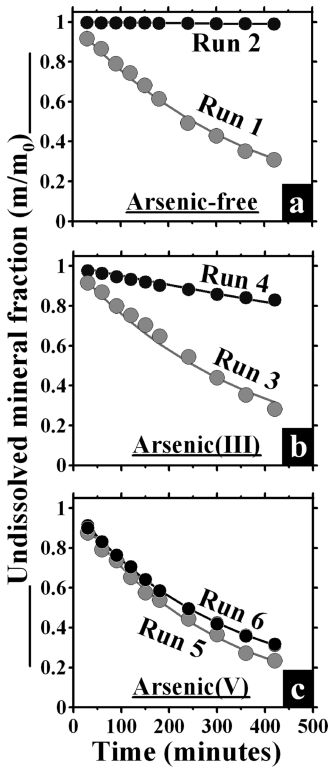

FIGURE 6. Reductive dissolution of the final solid-phase material in (a) runs 1 and 2, (b) runs 3 and 4, and (c) runs 5 and 6 as a function of time according to the method of Larsen and Postma (*30*).

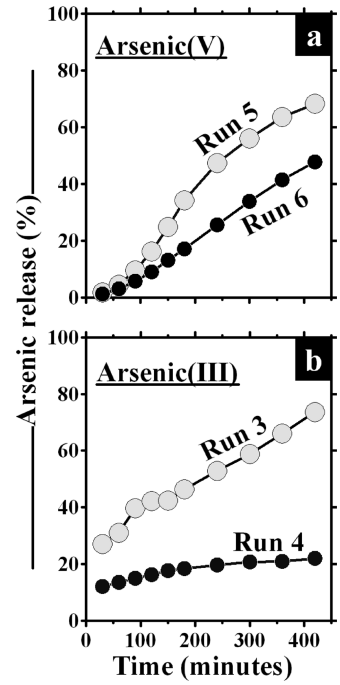

FIGURE 7. Arsenic release (expressed as % of total solid-phase arsenic) during the Fe(III)-reductive dissolution of the final solid-phase material resulting from (a) runs 5 and 6 and (b) runs 3 and 4.

As(III) concentration in run 4 was 16.5 ± 0.4 μM compared with only 11.2 ± 0.7 μM in run 3 (Figure 1). This suggests that the goethite formed in run 4 had a slightly lower affinity for As(III) compared with the precursor schwertmannite. However, given that the final As(III) concentrations in both run 4 and run 3 were much lower than the initial 1000 μM concentrations, the degree of As(III) desorption resulting from Fe(II)-catalyzed schwertmannite transformation was relatively small.

The aqueous As(V) concentrations did not differ significantly between runs 5 and 6 (Figure 1). This is consistent with the effect of As(V) in retarding the Fe(II)-catalyzed transformation of schwertmannite to goethite. As a result of this effect, there was little mineralogical difference between runs 5 and 6 (Figures 3 and 4), and thus negligible difference in the As(V) sorption affinity.

Reductive Dissolution and Associated Arsenic Mobilization. Under natural conditions, the Fe(II)-catalyzed transformation of schwertmannite to goethite is initiated by Fe(II) produced via reductive dissolution of Fe(III) (*21*). This can occur as a result of bacterially mediated Fe(III) reduction or abiotic reduction of Fe(III) by S(-II). Since these processes may eventually lead to reductive dissolution of the initial schwertmannite and neo-formed goethite, we examined reductive dissolution of the products of runs 1−6 using the ascorbic acid method of Larson and Postma (*30*). This method, which does not alter the arsenic oxidation state, is based on the abiotic reduction of solid-phase Fe(III) via electron transfer from ascorbic acid (*31*). Since the ascorbic acid extraction is carried out at pH 3, the liberated Fe(II) remains in solution and provides a measure of the extent of reductive dissolution of the Fe(III) solid-phase (*30, 31*).

In runs 1, 3, 5, and 6, the kinetics of reductive dissolution of the final Fe(III) solid-phase material were similar (Table 1, Figure 6). This can be attributed to the similar final mineralogy in these experimental runs, since there was little or no transformation of the original schwertmannite (Figures 3 and 4). In contrast, the extensive transformation of schwertmannite to goethite in runs 2 and 4 had a considerable effect on reductive dissolution of the final solid-phase material (Figure 6). In the case of run 2, the formation of highly crystalline goethite decreased the initial reductive dissolution rate (k') of the final solid-phase by more than 2 orders of magnitude relative to run 1 (Table 1). Likewise, comparison of the k' values for runs 3 and 4 shows almost an order of magnitude decrease in the final solid-phase reactivity due to the partial Fe(II)-catalyzed transformation of As(III)-sorbed schwertmannite (Table 1).

Arsenic release as a result of the reductive dissolution of the Fe(III) solid-phases described above are presented in Figure 7. For the As(V) treatments (runs 5 and 6), the release of arsenic displayed a sigmoidal trend as a function of time (Figure 7a). In the As(III) treatments (runs 3 and 4), a fast initial (0−30 min) release of solid-phase arsenic was followed by a more linear increase over time as the Fe(III) solid-phase experienced progressive reductive dissolution (Figure 7b). The observed trends in arsenic release can be attributed primarily to the progressive reductive dissolution of the Fe(III) solid-phase (with a consequent progressive decrease in the number of arsenic sorption sites).

The fast initial As(III) release triggered by the pH 3 ascorbic acid solution (Figure 7) is consistent with the pH-dependent solid/solution partitioning of As(III) with schwertmannite. For example, Burton et al. (*11*) reported a much greater tendency of As(III) to partition to the aqueous-phase at low pH compared to near-neutral pH. Hence, the initial (0−30 min) release of As(III) from the solid-phase produced in runs 3 and 4 following resuspension in the pH 3 ascorbic acid solution was probably mainly due to rapid pH-dependent As(III) desorption (as opposed to bulk mineral dissolution).

As shown in Figure 7, the release of arsenic as a result of Fe(III) reductive dissolution of the final solid-phase was greatest in runs 3 and 5. Both of these runs did not receive additions of Fe(II) and consequently experienced zero transformation of schwertmannite over the 9-day reaction period. As such, the low level of arsenic release from the final solid-phase of runs 4 and 6 is consistent with partial

transformation of schwertmannite to goethite in these runs (72% and 6%, respectively) and the greater resistance of the newly formed goethite to reductive dissolution.

General Discussion. A key finding from this study is the contrasting effects of As(V) and As(III) on schwertmannite transformation via the Fe(II)-pathway. In accord with previous studies on the slow, oxic transformation of schwertmannite (*4*, *26*), the presence of As(V) was found to substantially stabilize schwertmannite against Fe(II)-catalyzed transformation. The present study shows that As(III) also slows Fe(II)-catalyzed schwertmannite transformation relative to an absence of arsenic. However, the effect of As(III) is minor compared with the more substantial stabilizing effect of As(V). This may be a function of the weaker bonding of As(III) to schwertmannite sorption sites relative to that of As(V) under the pH conditions and arsenic loadings examined here (*11*).

We initially thought that the Fe(II)-catalyzed transformation of schwertmannite to goethite might enhance arsenic mobilization by driving desorption processes. While some desorption was apparent from the increase in aqueous As(III) in run 4, the overall extent of desorption was very minor. At the end of the reaction period for run 4, solid-phase As(III) decreased by only about 1% as a result of schwertmannite transformation. Thus, the Fe(II)-catalyzed transformation of schwertmannite to goethite is unlikely to be a major process contributing to enhanced arsenic mobility. In contrast, schwertmannite transformation to goethite substantially decreased the tendency for mobilization of arsenic via Fe(III)-reductive dissolution. Similar results have been observed during the Fe(II)-catalyzed transformation of As(V)-sorbed ferrihydrite (*24*) and have been attributed to arsenic being occluded within the newly formed goethite. Overall, the results suggest that Fe(II)-catalyzed transformation of schwertmannite to goethite may help to stabilize solid-phase arsenic and retard its subsequent release to groundwater.

Acknowledgments

Funding was provided by the Australian Research Council (grants DP0772050 and DP0666334) and the NSRRC in Taiwan. We thank Dr. Jyh-Fu Lee, of the NSRRC, for technical assistance and expert advice with the XAS data collection. The XPS work was conducted at the University of Queensland Centre for Microscopy and Microanalysis, under the expert guidance of Dr. Barry Wood.

Literature Cited

(1) Bigham, J. M.; Schwertmann, U.; Pfab, G. Influence of pH on mineral speciation in a bioreactor simulating acid mine drainage. *Appl. Geochem.* **1996**, *11*, 845–849.

(2) Bigham, J. M.; Schwertmann, U.; Traina, S. J.; Winland, R. L.; Wolf, M. Schwertmannite and the chemical modeling of iron in acid sulfate waters. *Geochim. Cosmochim. Acta* **1996**, *60*, 2111–2121.

(3) Carlson, L.; Bigham, J. M.; Schwertmann, U.; Kyek, A.; Wagner, F. Scavenging of As from acid mine drainage by schwertmannite and ferrihydrite: A comparison with synthetic analogues. *Environ. Sci. Technol.* **2002**, *36*, 1712–1719.

(4) Fukushi, K.; Sasaki, M.; Sato, T.; Yanasa, N.; Amano, H.; Ikeda, H. A natural attenuation of arsenic in drainage from an abandoned arsenic mine dump. *Appl. Geochem.* **2003**, *18*, 1267–1278.

(5) Regenspurg, S.; Brand, A.; Peiffer, S. Formation and stability of schwertmannite in acidic mining lakes. *Geochim. Cosmochim. Acta* **2004**, *68*, 1185–1197.

(6) Sullivan, L. A.; Bush, R. T. Iron precipitate accumulations associated with waterways in drained coastal acid sulfate landscapes of eastern Australia. *Mar. Freshwater Res.* **2004**, *55*, 727–736.

(7) Jonsson, J.; Persson, P.; Sjoberg, S.; Lovgren, L. Schwertmannite precipitated from acid mine drainage: phase transformation, sulphate release and surface properties. *Appl. Geochem.* **2005**, *20*, 179–191.

(8) Burton, E. D.; Bush, R. T.; Sullivan, L. A. Sedimentary iron geochemistry in acidic waterways associated with coastal lowland acid sulfate soils. *Geochim. Cosmochim. Acta* **2006**, *70*, 5445–5468.

(9) Fukushi, K.; Sato, T.; Yanase, N. Solid-solution reactions in As(V) sorption by schwertmannite. *Environ. Sci. Technol.* **2003**, *37*, 3581–3586.

(10) Fukushi, K.; Sato, T.; Yanase, N.; Minato, J.; Yamada, H. Arsenate sorption on schwertmannite. *Am. Mineral.* **2004**, *89*, 1728–1734.

(11) Burton, E. D.; Bush, R. T.; Johnston, S. G.; Watling, K.; Hocking, R. K.; Sullivan, L. A.; Heber, G. K. Sorption of arsenic(V) and arsenic(III) to schwertmannite. *Environ. Sci. Technol.* **2009**, *43*, 9202–9207.

(12) Acero, P.; Ayora, C.; Torrento, C.; Nieto, J.-M. The behaviour of trace elements during schwertmannite precipitation and subsequent transformation into goethite and jarosite. *Geochim. Cosmochim. Acta* **2006**, *70*, 4130–4139.

(13) Courtin-Nomade, A.; Grosbois, C.; Bril, H.; Roussel, C. Spatial variability of arsenic in some iron-rich deposits generated by acid mine drainage. *Appl. Geochem.* **2005**, *20*, 383–396.

(14) Schroth, A. W.; Parnell, R. A. Trace metal retention through the schwertmannite to goethite transformation as observed in a field setting, Alta Mine, MT. *Appl. Geochem.* **2005**, *20*, 907–917.

(15) Garcia, I.; Diez, M.; Martin, F.; Simon, M.; Dorronsoro, C. Mobility of arsenic and heavy metals in a sandy-loam textured and carbonated soil. *Pedosphere* **2009**, *19*, 166–175.

(16) Collins, R. N.; Jones, A. M.; Waite, T. D. Schwertmannite stability in acidified coastal environments. *Geochim. Cosmochim. Acta* **2010**, *74*, 482–496.

(17) Kumpulainen, S.; Carlson, L.; Raisanen, M. L. Seasonal variations of ochreous precipitates in mine effluents in Finland. *Appl. Geochem.* **2007**, *22*, 760–777.

(18) Peine, A.; Tritschler, A.; Kusel, K.; Peiffer, S. Electron flow in an iron-rich sediment - evidence for an acidity-driven iron cycle. *Limnol. Oceanogr.* **2000**, *45*, 1077–1087.

(19) Knorr, K. H.; Blodau, C. Controls on schwertmannite transformation rates and products. *Appl. Geochem.* **2007**, *22*, 2006–2015.

(20) Burton, E. D.; Bush, R. T.; Sullivan, L. A.; Mitchell, D. R. G. Reductive transformation of iron and sulfur in schwertmannite-rich accumulations associated with acidified coastal lowlands. *Geochim. Cosmochim. Acta* **2007**, *71*, 4456–4473.

(21) Burton, E. D.; Bush, R. T.; Sullivan, L. A.; Mitchell, D. R. G. Schwertmannite transformation to goethite via the Fe(II) pathway: Reaction rates and implications for iron-sulfide formation. *Geochim. Cosmochim. Acta* **2008**, *72*, 4551–4564.

(22) Burton, E. D.; Bush, R. T.; Sullivan, L. A.; Johnston, S. G.; Hocking, R. K. Mobility of arsenic and selected metals during re-flooding of iron- and organic-rich acid-sulfate soil. *Chem. Geol.* **2008**, *253*, 64–73.

(23) Johnston, S. G.; Burton, E. D.; Bush, R. T.; Keene, A. F.; Sullivan, L. A.; Smith, C. D.; McElnea, A. E.; Ahern, C. R.; Powell, B. Abundance and fractionation of Al, Fe and trace metals following tidal inundation of a tropical acid sulfate soil. *Appl. Geochem.* **2010**, *25*, 323–335.

(24) Gagliano, W. B.; Brill, M. R.; Bigham, J. M.; Jones, F. S.; Traina, S. J. Chemistry and mineralogy of ochreous sediments in a constructed mine drainage wetland. *Geochim. Cosmochim. Acta* **2004**, *68*, 2119–2128.

(25) Knorr, K. H.; Blodau, C. Experimentally altered groundwater inflow remobilizes acidity from sediments of an iron rich and acidic lake. *Environ. Sci. Technol.* **2006**, *40*, 2944–2950.

(26) Regenspurg, S.; Peiffer, S. Arsenate and chromate incorporation in schwertmannite. *Appl. Geochem.* **2005**, *20*, 1226–1239.

(27) Dhar, R. K.; Zheng, Y.; Rubenstone, J.; van Geen, A. A rapid colorimetric method of measuring arsenic concentrations in groundwater. *Anal. Chim. Acta* **2004**, *526*, 203–209.

(28) Ravel, B.; Newville, M. ATHENA, ARTEMIS, HEPHAESTUS: data analysis for X-ray absorption spectroscopy using IFEFFIT. *J. Synchrotron. Radiat.* **2005**, *12*, 537–541.

(29) Nesbit, H. W.; Muir, J.; Prawn, A. R. Oxidation of arsenopyrite by air and air-saturated distilled water, and implications for the mechanism of oxidation. *Geochim. Cosmochim. Acta* **1995**, *59*, 1773–1786.

(30) Larsen, O.; Postma, D. Kinetics of reductive bulk dissolution of lepidocrocite, ferrihydrite, and goethite. *Geochim. Cosmochim. Acta* **2001**, *65*, 1367–1379.

(31) Pedersen, H. D.; Postma, D.; Jakobsen, R. Release of arsenic associated with the reduction and transformation of iron oxides. *Geochim. Cosmochim. Acta* **2006**, *70*, 4116–4129.

ES903424H